



Fabrication of oxidation-resistant β -FeSi₂ film on Mg₂Si by RF magnetron-sputtering deposition

Jun-ichi Tani*, Masanari Takahashi, Hiroyasu Kido

Department of Electronic Materials, Osaka Municipal Technical Research Institute, 1-6-50 Morinomiya, Joto-ku, Osaka 536-8553, Japan

ARTICLE INFO

Article history:

Received 10 August 2009

Received in revised form 24 August 2009

Accepted 25 August 2009

Available online 31 August 2009

Keywords:

Intermetallics

Oxidation

Kinetics

Scanning electron microscopy

SEM

X-ray diffraction

ABSTRACT

We study the oxidation of Mg₂Si and analyze its kinetics using the Johnson–Mehl–Avrami (JMA) equation. Above 450 °C, Mg₂Si reacts with O₂ in air to yield MgO and Si. The Avrami exponent (*n*) is equal to ~0.5, and it depends on the reaction temperature and time; this indicates that the oxidation is controlled by the diffusion-controlled reaction. In order to improve the oxidation-resistance of Mg₂Si, β -FeSi₂ films were fabricated on sintered Mg₂Si samples by RF magnetron-sputtering deposition at RT followed by post-annealing at 600 °C in vacuum. An oxide layer having a thickness of $8 \pm 3 \mu\text{m}$ was observed on the uncoated Mg₂Si samples after heat treatment in air at 600 °C for 3 h. However, no oxide layer was formed on Mg₂Si samples coated with 0.7- μm thick β -FeSi₂ films. The β -FeSi₂ layer effectively prevented the diffusion of oxygen at 600 °C and improved the oxidation-resistance of Mg₂Si.

© 2009 Elsevier B.V. All rights reserved.

1. Introduction

The intermetallic compound Mg₂Si has been considered as a potential environment-friendly high-performance thermoelectric material [1–12], because it is non-toxic, lightweight, and it has high electron mobility; in addition, the raw materials used to manufacture it are inexpensive. Thermoelectric materials should have a large Seebeck coefficient *S*, small electrical resistivity ρ , and small thermal conductivity κ . Impurity doping drastically affects the thermoelectric properties of Mg₂Si and its solid solution, and therefore, it is essential to determine suitable dopants for Mg₂Si. In many experimental studies, Mg₂Si has been doped with impurities with the objective of improving its thermoelectric figure of merit *Z*.

Oxidation is one of the primary mechanisms for the degradation of high-temperature Mg₂Si thermoelectric devices. However, few studies have attempted to clarify this mechanism. Therefore, it is essential to understand the oxidation mechanism of Mg₂Si in order to develop new oxidation-resistant films. β -FeSi₂ has an orthorhombic structure (space group: *Cmca*), and it is also an environment-friendly silicide semiconductor [13]. Moreover, β -FeSi₂ exhibits excellent oxidation-resistance in the high-temperature region below 800 °C [14,15]. Therefore, β -FeSi₂ can be considered as a potential candidate for use as an oxidation-resistant coating material for Mg₂Si. The formation of β -FeSi₂ films

has been attempted using various methods, and it has been successfully formed on a glass plate, Si single crystal, and polycrystalline alumina by the RF magnetron-sputtering method [16–22].

In the present study, we investigate the oxidation of Mg₂Si and analyze its kinetics using the Johnson–Mehl–Avrami (JMA) equation. In order to improve the oxidation-resistance of Mg₂Si, β -FeSi₂ films were fabricated on sintered Mg₂Si samples by RF magnetron-sputtering deposition and then the oxidation-resistance of the samples was evaluated.

2. Experimental

0.5 g of Mg₂Si powder (purity: >99.5%; size: <20 mesh; Mitsuwa Chemical Co., Osaka, Japan) was pressed into pellets (diameter: 13 mm) at 60 MPa using a hand press and then fired in air to 200–800 °C with dwell times of 6 min to 4 h in an open crucible. The heating rate was 20 °C/min. Sintered dense Mg₂Si samples were fabricated using the spark plasma sintering (SPS) method [7–13]. The constituent Mg (purity: >99.9%; size: <180 μm ; Kojundo Chemical Laboratory Co. Ltd.; Saitama, Japan) and Si (purity: >99.999%; size: <75 μm , Kojundo Chemical Laboratory Co., Ltd.; Saitama, Japan) powders were ground together and then heated at 1053 K for 10 min at 20 MPa in a graphite die (diameter: 30 mm) in vacuum (<4 Pa) by the SPS method at a heating rate of ~50 K/min. The density of the annealed samples was more than 99% of the theoretical value. The surfaces of the sintered Mg₂Si samples were polished with a 1200 grid SiC paper prior to sputtering. Fe–Si films were deposited by RF magnetron-sputtering (sputtering power: 400 W; model HSR-551S, Shimadzu Corporation, Kyoto, Japan) on the Mg₂Si sample (temperature: RT) under an Ar atmosphere (pressure: 0.133 Pa). The sputtering target was a polycrystalline β -FeSi₂ disk (diameter: 100 mm).

The Fe–Si films and the oxidation of the sintered Mg₂Si samples were characterized by using a scanning electron microscope (model JSM-6460LA, JEOL, Tokyo, Japan) at 20 kV with a working distance 20 mm. A phase analysis was carried out by X-ray powder diffraction (XRD; model RINT 2500, Rigaku, Tokyo) using CuK α radi-

* Corresponding author. Tel.: +81 6 6963 8081; fax: +81 6 6963 8099.
E-mail address: tani@omtri.city.osaka.jp (J.-i. Tani).

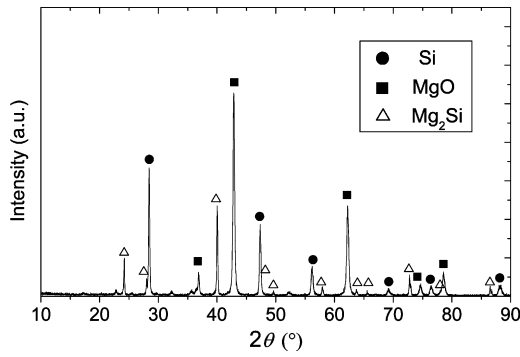


Fig. 1. XRD patterns of products obtained by firing of Mg₂Si pellet in air at 800 °C for 12 h.

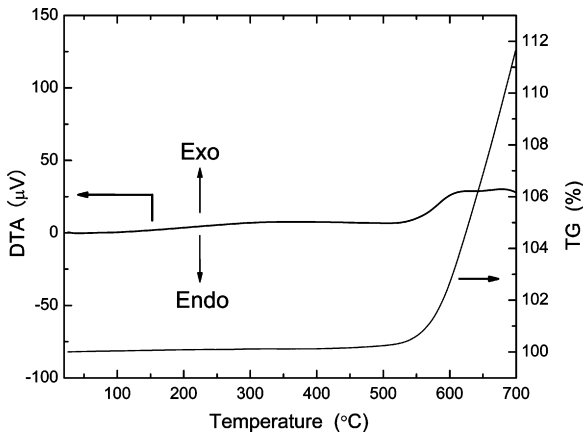


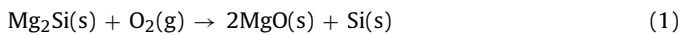
Fig. 2. TG/DTA curves of Mg₂Si in air at a heating rate of 10 °C/min.

ation at 40 kV and 50 mA. Phase identification was accomplished by comparing the experimental XRD patterns with the standards compiled by the International Center for Diffraction Data (ICDD). In order to study the oxidation mechanism of Mg₂Si in detail, thermogravimetric analysis and differential thermal analysis (TGA/DTA; model TGA/DTA 320, Seiko Instruments Inc., Chiba, Japan) of the Mg₂Si powder was carried out at a heating rate of 10 °C/min in air flowing at 300 ml/min. The thermal expansion of sintered dense Mg₂Si, fabricated by the SPS method, was measured on a bar (4 mm × 4 mm × 13 mm) using a thermal mechanical analyzer (model TMA 8310, Rigaku, Tokyo, Japan) in N₂ flowing at 100 ml/min at a heating rate of 5 °C/min in the temperature range of 25–300 °C.

3. Results and discussion

3.1. Oxidation behavior of Mg₂Si

Fig. 1 shows XRD patterns of the products obtained by the firing of a Mg₂Si pellet in air at 800 °C for 12 h. The XRD analyses revealed the presence of MgO (ICDD Card #45-0946), Si (ICDD Card #27-1402), and unreacted Mg₂Si (ICDD Card #35-0773). The following reaction occurred between Mg₂Si and O₂ at 450 °C:



At the beginning of the reaction, the outer portions of the pellets were brown, suggesting that a Si phase had formed, and the inside of the pellet was blue-black, which is characteristic of Mg₂Si.

Fig. 2 shows TGA/DTA curves of Mg₂Si obtained under air flowing at a rate of 300 ml/min and at a heating rate of 10 °C/min. The weight of Mg₂Si remained constant below ~450 °C. The majority of the weight gain of Mg₂Si occurred above ~500 °C due to the oxidation reaction. Our DTA result is in good agreement with previous experimental results [23,24].

The reaction kinetics of the oxidation mechanism was examined. Hancock and Sharp [25] proposed the application of the

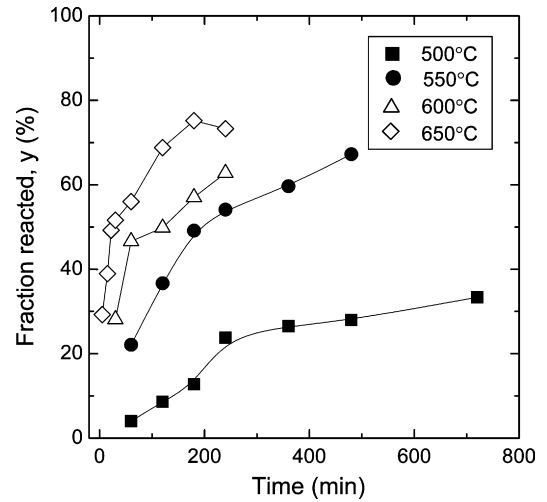


Fig. 3. Fraction reacted, *y*, as a function of reaction time at various temperatures during oxidation of Mg₂Si.

generalized Avrami formula [26–28] to the study of solid-state kinetics data. In general, the Johnson–Mehl–Avrami (JMA) kinetics equation is given by:

$$y = 1 - \exp[-(kt)^n], \quad (2)$$

where *y* is the fraction reacted at a given temperature in time *t*; *k*, the reaction rate constant; and *n*, the Avrami exponent.

$$k = A \exp\left(-\frac{E_a}{RT}\right); \quad (3)$$

here, *k* is related to the activation energy of the process, *E_a*, through the Arrhenius temperature dependence.

The logarithmic equation that results from the rearrangement of Eq. (2) is

$$\ln\left[\ln\left(\frac{1}{1-y}\right)\right] = n \ln k + n \ln t, \quad (4)$$

where *y* was determined using Eq. (5) by measuring the weight of the pellet before and after firing in air.

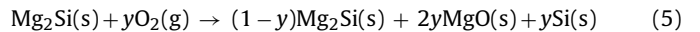


Fig. 3 shows the reacted fraction as a function of the reaction time of Mg₂Si oxidation. The reacted fraction increases with

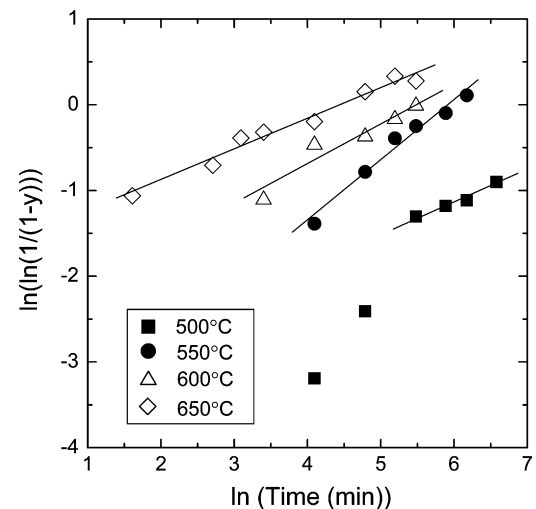


Fig. 4. Reaction kinetics fitted by the Johnson–Mehl–Avrami equation for the oxidation of Mg₂Si.

increasing with reaction time and temperature. The reacted fractions at 500, 550, 600, and 650 °C at a dwell time of 2 h are 8.6, 36.7, 49.8, and 68.8%, respectively. Fig. 4 shows that the plot of the $\ln[\ln(1/(1-y))]$ vs. $\ln(\text{time})$ for Mg_2Si oxidation is a straight line at the fraction reacted above ~20%. The values of n for reaction temperatures of 500, 550, 600, and 650 °C are 0.36, 0.71, 0.48, and 0.36, respectively. From the slope of the $\ln k-1/T$ plot, the activation energy E_a is determined to be 177 kJ/mol. A value close to 0.5 indicates that the rate-controlling step is a diffusion mechanism [25,29]. Therefore, it is important to block the diffusion of oxygen onto the surface of Mg_2Si in order to prevent the oxidation of Mg_2Si .

3.2. $\beta\text{-FeSi}_2$ film deposited on sintered Mg_2Si samples by RF magnetron-sputtering method

In order to improve the oxidation-resistance of Mg_2Si , $\beta\text{-FeSi}_2$ films were fabricated on sintered Mg_2Si samples by RF magnetron-sputtering deposition at room temperature (RT) followed by post-annealing at 600 °C for 1 h in vacuum. Fig. 5 shows XRD patterns of Fe–Si film deposited on sintered Mg_2Si samples before and after annealing at 600 °C for 1 h in vacuum (<0.1 Pa). No XRD diffraction peaks except those of the Mg_2Si phase are observed in the as-sputtered samples, indicating that Fe–Si films deposited at RT have an amorphous structure. After annealing at 600 °C, the diffraction peaks of the $\beta\text{-FeSi}_2$ phase as well as Mg_2Si phase are detected in the XRD pattern. The coefficient of thermal expansion (CTE) of SPS-sintered polycrystalline Mg_2Si in the temperature range of 25–300 °C is $16.5 \times 10^{-6} \text{ °C}^{-1}$; this value is much higher than that of $\beta\text{-FeSi}_2$ ($7.7 + 5.5 \times 10^{-3} T) \times 10^{-6} \text{ °C}^{-1}$ (T = absolute temperature) [30]. Scanning electron microscopy analysis of the surface of $\beta\text{-FeSi}_2$ films deposited on sintered Mg_2Si samples indicates that peeling or partial removal of film occurs when the films are thicker than 1 μm because of the difference between the CTE values of $\beta\text{-FeSi}_2$ and Mg_2Si . No peeling or partial removal of film was observed when the film thickness was 0.7 μm .

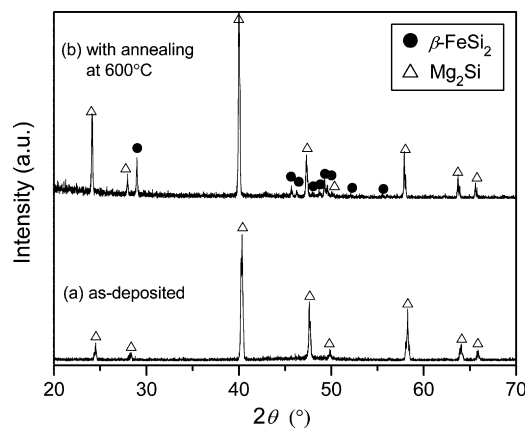


Fig. 5. XRD patterns of Fe–Si films deposited on sintered Mg_2Si samples with and without annealing at 600 °C in vacuum: (a) as-deposited; and (b) with annealing at 600 °C for 1 h.

Fig. 6 shows scanning electron micrographs of the cross-sections of sintered Mg_2Si samples with and without $\beta\text{-FeSi}_2$ films after heat treatment in air at 600 °C for 1–3 h. The thickness of the oxide layer that was formed on the uncoated Mg_2Si samples was $5 \pm 2 \mu\text{m}$ and $8 \pm 3 \mu\text{m}$ after 1 and 3 h, respectively. The surface of sintered Mg_2Si samples was brown, suggesting the formation of Si phase. The oxide layer was composed of Si and MgO , and it had a very small grain size of $< \sim 200 \text{ nm}$. Because the oxide layer was porous, the oxidation reaction proceeded through the diffusion of oxygen at the interface between Mg_2Si and the oxide layer.

However, in case of the Mg_2Si samples coated with 0.7 μm thick $\beta\text{-FeSi}_2$ films, no oxide layer was formed after heat treatment at 600 °C in air for 1–3 h. Scanning electron microscopy analysis of the surface of the $\beta\text{-FeSi}_2$ films coated on sintered Mg_2Si samples indicated the absence of pinholes and cracks. Therefore, we can conclude that the $\beta\text{-FeSi}_2$ layer effectively prevented the diffusion

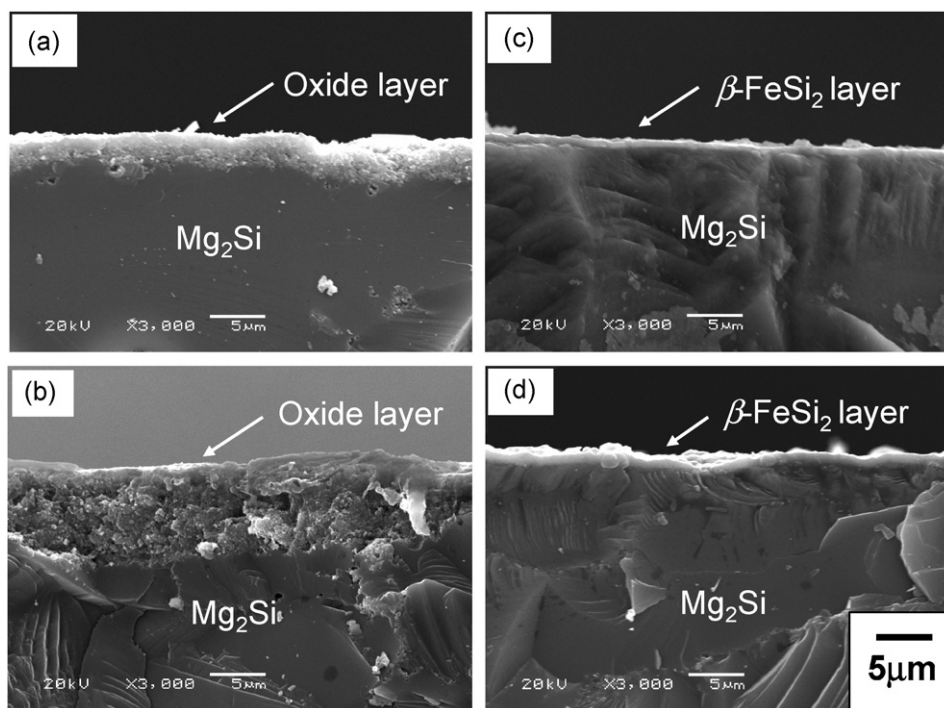


Fig. 6. Scanning electron micrographs of cross-sections of sintered Mg_2Si samples with and without $\beta\text{-FeSi}_2$ films after heat treatment in air at 600 °C for 1–3 h: (a) without $\beta\text{-FeSi}_2$ films for 1 h; (b) without $\beta\text{-FeSi}_2$ films for 3 h; (c) with $\beta\text{-FeSi}_2$ films for 1 h; and (d) with $\beta\text{-FeSi}_2$ films for 3 h.

of oxygen at 600 °C, and it improved the oxidation-resistance of Mg₂Si.

4. Conclusions

Above 450 °C, Mg₂Si reacts with O₂ in air to yield MgO and Si. The Avrami exponent (*n*) is equal to ~0.5, and it depends on the reaction temperature and time; this indicates that the oxidation is controlled by the diffusion-controlled reaction. In order to improve the oxidation-resistance of Mg₂Si, β-FeSi₂ films were fabricated on sintered Mg₂Si samples by RF magnetron-sputtering deposition at RT followed by post-annealing at 600 °C in vacuum. An oxide layer having a thickness of 8 ± 3 μm was observed on the uncoated Mg₂Si samples after heat treatment in air at 600 °C for 3 h. However, no oxide layer was formed on Mg₂Si samples coated with 0.7-μm thick β-FeSi₂ films. The β-FeSi₂ layer effectively prevented the diffusion of oxygen at 600 °C and improved the oxidation-resistance of Mg₂Si.

Acknowledgements

This research was partially supported by Grants-in-Aid, for Young Scientists (B), No. 18760514, 2007 from the Ministry of Education, Sports, and Culture, Science and Technology (MEXT) and Research for Promoting Technological Seeds (A), No. 11-029, 2008, from the Japan Science and Technology Agency (JST).

References

- [1] C.B. Vining, in: D.M. Rowe (Ed.), CRC Handbook of Thermoelectrics, CRC Press, New York, 1995, p. 277.
- [2] V.K. Zaitsev, M.I. Fedorov, I.S. Eremin, E.A. Gurieva, in: D.M. Rowe (Ed.), Thermoelectrics Handbook Macro to Nano, CRC Press, New York, 2006, Chapter 29.
- [3] V.K. Zaitsev, M.I. Fedorov, E.A. Gurieva, I.S. Eremin, P.P. Kondtantinov, A.Yu. Samunin, M.V. Vedernikov, Phys. Rev. B 74 (2006) 045207.
- [4] Y. Noda, H. Kon, Y. Furukawa, N. Otsuka, I.A. Nishida, K. Masumoto, Mater. Trans. JIM 33 (1992) 845.
- [5] Y. Noda, H. Kon, Y. Furukawa, N. Otsuka, I.A. Nishida, K. Masumoto, Mater. Trans. JIM 33 (1992) 851.
- [6] M. Akasaka, T. Iida, A. Matsumoto, K. Yamanaka, T. Takanashi, T. Imai, N. Hamada, J. Appl. Phys. 104 (2008) 013703.
- [7] T. Kajikawa, K. Shida, S. Sugihara, M. Ohmori, T. Hirai, Proc. 16th Int. Conf. on Thermoelectrics (ICT'97), 1997, p. 275.
- [8] M. Umamoto, Y. Shirai, K. Tsuchiya, Proceedings of the 4th Pacific Rim International Conference on Advanced Materials and Processing (PRICM4), 2001, p. 2145.
- [9] J. Tani, H. Kido, Physica B 364 (2005) 218.
- [10] J. Tani, H. Kido, Jpn. J. Appl. Phys. Part 1 46 (2007) 3309.
- [11] J. Tani, H. Kido, Intermetallics 15 (2007) 1202.
- [12] J. Tani, H. Kido, J. Alloys. Compd. 466 (2008) 335.
- [13] H. Lange, Phys. Stat. Sol. (b) 201 (1997) 3.
- [14] S. Chang, M. Nakano, K. Matsumaru, K. Ishizaki, M. Takeda, J. Jpn. Inst. Metals 70 (2006) 20.
- [15] K. Uemura, I. Nishida, Thermoelectric Semiconductors and their applications, Nikkan-Kogyo, Tokyo, 1988, p. 178 in Japanese.
- [16] M. Komabayashi, K. Hijikata, S. Ido, Jpn. J. Appl. Phys. 29 (1990) 1118.
- [17] T. Tsunoda, M. Mukaida, A. Watanabe, Y. Imai, J. Mater. Res. 11 (1996) 2062.
- [18] K. Okajima, C. Wen, M. Ihara, I. Sakata, K. Yamada, Jpn. J. Appl. Phys. 38 (1999) 781.
- [19] T. Yoshitake, T. Hanada, K. Nagayama, J. Mater. Sci. Lett. 19 (2000) 537.
- [20] H. Kamata, H. Anzai, M. Sugita, Y. Oikawa, H. Ozaki, Proceedings of the 22th International Conference on Thermoelectrics (ICT'03), 2003, p. 391.
- [21] N. Momose, Y. Hashimoto, K. Ito, Jpn. J. Appl. Phys. Part 1 42 (2003) 5490.
- [22] Y. Okada, N. Momose, M. Takahashi, Y. Hashimoto, K. Ito, Jpn. J. Appl. Phys. Part 1 44 (2005) 6505.
- [23] J.M. Muñoz-Palos, M.C. Cristina, P. Adeva, Mater. Trans. JIM 37 (1996) 1602.
- [24] M. Riffel, J. Schilz, Proceedings of the 16th International Conference on Thermoelectrics (ICT'97), 1997, p. 283.
- [25] J.D. Hancock, J.H. Sharp, J. Am. Ceram. Soc. 55 (1972) 74.
- [26] M. Avrami, J. Chem. Phys. 7 (1939) 1103.
- [27] M. Avrami, J. Chem. Phys. 8 (1940) 212.
- [28] M. Avrami, J. Chem. Phys. 9 (1941) 177.
- [29] S.F. Hulbert, Br. Ceram. Soc. J. 6 (1967) 11.
- [30] L.P. Andreeva, P.V. Geld, Izvestiya VUZov, Chernaya Metall. N2 (1965) 111.